

# Calcium channel $\beta$ subunits differentially modulate recovery of the channel from inactivation

Michael C. Jeziorski<sup>a,1</sup>, Robert M. Greenberg<sup>a,b</sup>, Peter A.V. Anderson<sup>a,b,c,\*</sup>

<sup>a</sup>The Whitney Laboratory, University of Florida, 9505 Ocean Shore Blvd., St. Augustine, FL 32086, USA

<sup>b</sup>Department of Neuroscience, University of Florida, 9505 Ocean Shore Blvd., St. Augustine, FL 32086, USA

<sup>c</sup>Department of Physiology, University of Florida, 9505 Ocean Shore Blvd., St. Augustine, FL 32086, USA

Received 18 August 2000; accepted 15 September 2000

Edited by Maurice Montal

**Abstract** We examined the effects of calcium channel  $\beta$  subunits upon the recovery from inactivation of  $\alpha_1$  subunits expressed in *Xenopus* oocytes. Recovery of the current carried by the L-type  $\alpha_1$  subunit (*cyCa<sub>v</sub>1*) from the jellyfish *Cyanea capillata* was accelerated by coexpression of any  $\beta$  subunit, but the degree of potentiation differed according to which  $\beta$  isoform was coexpressed. The *Cyanea*  $\beta$  subunit was most effective, followed by the mammalian  $\beta_3$ ,  $\beta_4$ , and  $\beta_{2a}$  subtypes. Recovery of the human *Ca<sub>v</sub>2.3* subunit was also modulated by  $\beta$  subunits, but was slowed instead.  $\beta_3$  was the most potent subunit tested, followed by  $\beta_4$ , then  $\beta_{2a}$ , which had virtually no effect. These results demonstrate that different  $\beta$  subunit isoforms can affect recovery of the channel to varying degrees, and provide an additional mechanism by which  $\beta$  subunits can differentially regulate  $\alpha_1$  subunits. © 2000 Federation of European Biochemical Societies. Published by Elsevier Science B.V. All rights reserved.

**Key words:** Voltage-gated calcium channel;  $\alpha_1$  subunit;  $\beta$  subunit; Inactivation; L-type current; R-type current

## 1. Introduction

In excitable cells, voltage-gated calcium channels form the link between membrane depolarization and the calcium influx that initiates intracellular processes. The kinetics of channel activation and inactivation are critical in determining the cellular response, and much current heterogeneity stems from the genetic diversity of channel subunits. At least 10 distinct mammalian forms of the  $\alpha_1$  subunit, the pore-forming subunit of the calcium channel, have been identified and categorized as either high voltage-activated (HVA) or low voltage-activated (LVA);  $\alpha_1$  subunits within these families differ considerably in the properties of the currents they gate. Further current variation results from modulation of the  $\alpha_1$  subunit by phosphorylation, G proteins, or auxiliary subunits. In HVA channels, the  $\alpha_1$  subunit is associated with auxiliary  $\beta$ ,

$\alpha_2\delta$ , and  $\gamma$  subunits, of which  $\beta$  subunits have the most profound regulatory effects.  $\beta$  Subunits modulate several parameters of  $\alpha_1$  activity, including level of channel expression, threshold of activation, rate of inactivation, and steady-state inactivation [1–3]. Four mammalian subtypes of the  $\beta$  subunit ( $\beta_1$ – $\beta_4$ ), as well as additional splice variants, have been cloned (for a review see [3]), and regulation of current properties may differ according to the type of  $\beta$  isoform present. For example, the  $\beta_{2a}$  subunit differs from the  $\beta_{1b}$ ,  $\beta_3$ , and  $\beta_4$  isoforms in its effects upon  $\alpha_1$  inactivation [4–6]. This variation is significant in that certain  $\alpha_1$  subunits have been shown to associate with multiple  $\beta$  subunits in vivo [7–9].

We have previously investigated the interactions between an  $\alpha_1$  and a  $\beta$  subunit cloned from the jellyfish *Cyanea capillata* [10]. The L-type calcium channel  $\alpha_1$  subunit (*cyCa<sub>v</sub>1*; previously called *CyCa $\alpha_1$* ) is modulated by the calcium channel  $\beta$  subunit (*cy $\beta$* ) in a manner that is consistent with interactions between mammalian calcium channel subunits. When coexpressed with *cyCa<sub>v</sub>1* in *Xenopus* oocytes, *cy $\beta$*  increases whole-cell current amplitude, shifts the current–voltage relationship to more hyperpolarized potentials, and alters the kinetics of current inactivation, actions that can be duplicated by coexpression of the mammalian  $\beta_{2a}$  subunit with *cyCa<sub>v</sub>1*. An additional component of the *Cyanea*  $\alpha_1$ – $\beta$  interaction is the ability of *cy $\beta$*  to accelerate the recovery of the channel from inactivation, a form of modulation that has not been reported for mammalian channels. The present experiments were designed to examine the effects of different  $\beta$  subunits on recovery of both *cyCa<sub>v</sub>1* and a mammalian  $\alpha_1$  subunit, the human R-type calcium channel *Ca<sub>v</sub>2.3* isoform (*hCa<sub>v</sub>2.3*; previously called  $\alpha_{1E}$ ).

## 2. Materials and methods

The cloning and functional expression of the *cyCa<sub>v</sub>1* [11] and *cy $\beta$*  [10] subunits have previously been described. All clones were transcribed using the T7 version of the mMessage mMachine kit (Ambion), and the amount and purity of transcribed RNA were determined by denaturation with glyoxal and gel electrophoresis. Oocytes were injected with a constant amount of  $\alpha_1$  RNA, combined either with  $\beta$  subunit RNA or with an equivalent volume of water. RNA was combined in a molar ratio of 1:3  $\alpha_1$ : $\beta$  RNA in order to ensure that the  $\beta$  subunit was present at saturating levels [6]. Oocytes were incubated for 3–7 days; because levels of channel expression change over time, recordings on any given day were made from oocytes in all treatment groups. Two-electrode voltage clamp recordings were conducted in a bath solution containing 40 mM Sr(OH)<sub>2</sub>, 40 mM *N*-methylglucamine, 10 mM glucose, and 10 mM HEPES, adjusted to pH 7.4 with methanesulfonic acid [12]. Sr<sup>2+</sup> was used as the charge carrier due to its high permeance of the *cyCa<sub>v</sub>1* subunit [11]. All oocytes were injected with 40 nl 100 mM BAPTA at least 1 h prior

\*Corresponding author. Fax: (1)-904-461 4008.  
E-mail: paa@whitney.ufl.edu

<sup>1</sup> Present address: Centro de Neurobiología, Universidad Nacional Autónoma de México, Campus Juriquilla, P.O. Box 1-1141, Querétaro, Qro. C.P. 76001, Mexico.

**Abbreviations:** *cyCa<sub>v</sub>1*, *Cyanea capillata* L-type calcium channel  $\alpha_1$  subunit; *hCa<sub>v</sub>2.3*, human R-type calcium channel (previously called  $\alpha_{1E}$ ); *cy $\beta$* , *Cyanea capillata* calcium channel  $\beta$  subunit; HVA, high voltage-activated; LVA, low voltage-activated

to recording to block the endogenous calcium-activated  $\text{Cl}^-$  current [13]. In experiments involving  $\text{cyCa}_v1$ , complete inactivation of the current was produced by a 1.5 s voltage prepulse from  $-110$  mV to  $+10$  mV, and recovery was determined by a 50 ms test pulse to  $+10$  mV after a hyperpolarizing step of varying duration or voltage. The human  $\text{Ca}_v2.3$  subunit was studied in the same manner, except that the length of the prepulse was 9.6 s (16.2 s when  $\text{Ca}_v2.3$  was coexpressed with  $\beta_{2a}$ , due to the slower rate of inactivation). In most instances, the extended prepulse inactivated the channel completely ( $<2\%$  of peak current remaining by the end of the prepulse), but when  $\text{hCa}_v2.3$  was coexpressed with  $\beta_{2a}$ , approximately 7% of the current remained at the end of the prepulse. For this reason, recovery was measured as (peak current elicited by test pulse—residual current at end of prepulse)/(peak current elicited by prepulse—residual current at end of prepulse). Successive episodes during a series of tests were separated by 30 s ( $\text{cyCa}_v1$ ) or 90 s ( $\text{hCa}_v2.3$ ); the amplitude of the current elicited by the prepulse after this delay demonstrated that the channel had completely recovered from inactivation.

### 3. Results

Because the purpose of the present experiments was to examine the effects of calcium channel  $\beta$  subunits upon the recovery from inactivation of  $\alpha_1$  subunits, we studied two  $\alpha_1$  subunits,  $\text{cyCa}_v1$  [11], and the human  $\text{Ca}_v2.3$  subunit [14], that produce robust, rapidly inactivating currents in oocytes in the absence of coexpressed  $\beta$  subunits. A consistent effect of  $\beta$  subunit modulation is a leftward shift in the current–voltage relationship of the  $\alpha_1$  subunit. Such a shift was seen for the  $\text{cyCa}_v1$  subunit in every instance in which a  $\beta$  subunit was coexpressed (Fig. 1A), demonstrating that each mammalian  $\beta$  subunit studied can regulate  $\text{cyCa}_v1$ . A similar, though smaller, shift in the  $\text{hCa}_v2.3$  curve was produced by coexpression of either  $\text{cy}\beta$  or the mammalian  $\beta$  subunits (Fig. 1B). The magnitude of the effect is comparable to that previously reported for the  $\text{hCa}_v2.3$  subunit [14].

Recovery from inactivation was measured by administering an extended prepulse to fully inactivate the current, then repolarizing the cell and measuring the current elicited by a test pulse after a certain delay. In this manner, recovery could be distinguished from phenomena such as facilitation or inactivation from intermediate closed states. The initial experiments investigated the time course of recovery after repolarization to  $-110$  mV. As other studies have shown [15,16], recovery of the calcium current is best fit by a biexponential function. The parameters of curves fit to individual experiments varied sig-

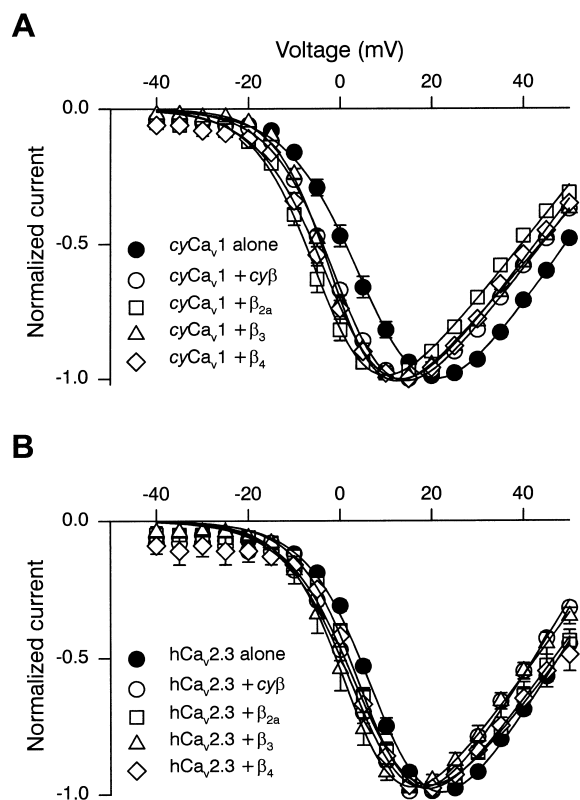


Fig. 1. A: Current–voltage relationships for  $\text{cyCa}_v1$  expressed alone or in the presence of the  $\text{cy}\beta$ ,  $\beta_{2a}$ ,  $\beta_3$ , or  $\beta_4$  subunits. Currents were measured in 40 mM  $\text{Sr}^{2+}$ . B: Current–voltage relationships for the human  $\text{Ca}_v2.3$  subunit in the absence and presence of  $\beta$  subunits.  $n = 7$ –10 cells.

nificantly, so curves were fit to mean values to provide an estimate of the fast and slow time constants of recovery. The faster component accounted for 40% of the recovery of the current carried by  $\text{cyCa}_v1$  (Fig. 2A and Table 1). Coexpression of any  $\beta$  subunit accelerated the recovery of  $\text{cyCa}_v1$ , though the degree of potentiation differed for each subunit.  $\text{cy}\beta$  had the greatest effect, followed by  $\beta_4$  and  $\beta_3$ , each of which decreased the time constants of both components of recovery. The  $\text{cy}\beta$  subunit also increased the proportion of recovery accounted for by the fast component, as did the

Table 1  
Parameters of curves fitted to data in Figs. 2 and 3

	Recovery after $-110$ mV interpulse			Recovery after $-60$ mV interpulse			Voltage dependence of recovery			
	$\tau_1$ (ms)	$\tau_2$ (ms)	$p_1$	$\tau_1$ (ms)	$\tau_2$ (ms)	$p_1$	max rec (%)	$k$	$V_{1/2}$ (mV)	min rec (%)
$\text{cyCa}_v1$	$312.4 \pm 30.5$	$2177 \pm 189$	$0.40 \pm 0.04$	$50.2 \pm 48.6$	$3850 \pm 257$	$0.06 \pm 0.02$	$0.42 \pm 0.02$	$18.1 \pm 1.4$	$-75.4 \pm 1.9$	$0.07 \pm 0.0$
$\text{cyCa}_v1 + \text{cy}\beta$	$135.2 \pm 13.1$	$1188 \pm 136$	$0.58 \pm 0.04$	$136.9 \pm 11.9$	$2277 \pm 221$	$0.49 \pm 0.02$	$0.68 \pm 0.03$	$12.8 \pm 1.6$	$-35.2 \pm 1.7$	$-0.01 \pm 0.03$
$\text{cyCa}_v1 + \beta_{2a}$	$382.6 \pm 78.4$	$2558 \pm 1372$	$0.63 \pm 0.14$	$98.8 \pm 20.3$	$3444 \pm 136$	$0.12 \pm 0.01$	$0.66 \pm 0.10$	$25.4 \pm 4.6$	$-77.9 \pm 6.5$	$0.03 \pm 0.02$
$\text{cyCa}_v1 + \beta_3$	$162.4 \pm 20.4$	$1398 \pm 120$	$0.43 \pm 0.04$	$142.4 \pm 19.4$	$2822 \pm 200$	$0.28 \pm 0.02$	$0.64 \pm 0.06$	$20.9 \pm 3.1$	$-38.7 \pm 2.9$	$-0.07 \pm 0.04$
$\text{cyCa}_v1 + \beta_4$	$141.0 \pm 21.1$	$1304 \pm 150$	$0.47 \pm 0.05$	$123.4 \pm 4.2$	$2636 \pm 57$	$0.33 \pm 0.01$	$0.65 \pm 0.05$	$19.6 \pm 3.0$	$-40.4 \pm 2.8$	$-0.03 \pm 0.04$
$\text{hCa}_v2.3$	$62.9 \pm 7.2$	$877 \pm 91$	$0.63 \pm 0.04$	$167.2 \pm 20.4$	$2270 \pm 85$	$0.21 \pm 0.02$	$0.78 \pm 0.06$	$17.9 \pm 2.3$	$-66.0 \pm 2.5$	$0.05 \pm 0.02$
$\text{hCa}_v2.3 + \text{cy}\beta$	$110.2 \pm 6.5$	$1190 \pm 103$	$0.64 \pm 0.02$	$256.7 \pm 84.3$	$6193 \pm 2031$	$0.27 \pm 0.06$	$0.80 \pm 0.04$	$17.1 \pm 1.2$	$-77.5 \pm 1.6$	$0.04 \pm 0.01$
$\text{hCa}_v2.3 + \beta_{2a}$	$86.7 \pm 8.5$	$1102 \pm 140$	$0.64 \pm 0.04$	$161.0 \pm 16.0$	$2707 \pm 110$	$0.24 \pm 0.01$	ND	ND	ND	ND
$\text{hCa}_v2.3 + \beta_3$	$115.0 \pm 6.1$	$1683 \pm 135$	$0.61 \pm 0.02$	$311.6 \pm 24.4$	$16290 \pm 2510$	$0.25 \pm 0.01$	$0.77 \pm 0.03$	$17.0 \pm 0.8$	$-82.7 \pm 1.3$	$0.00 \pm 0.00$
$\text{hCa}_v2.3 + \beta_4$	$90.3 \pm 12.5$	$1133 \pm 211$	$0.64 \pm 0.05$	$304.6 \pm 53.0$	$9458 \pm 3594$	$0.34 \pm 0.04$	$0.80 \pm 0.04$	$16.6 \pm 1.4$	$-71.4 \pm 1.6$	$0.02 \pm 0.01$

Recovery curves were fitted using a biexponential function: percent recovery =  $1 - p_1 \exp(-t/\tau_1) - (1 - p_1) \exp(-t/\tau_2)$ , where  $p_1$  and  $(1 - p_1)$  represent the proportion of recovery accounted for by the time constants  $\tau_1$  and  $\tau_2$ , respectively. The voltage dependence of recovery curves were fit by the Boltzmann function: percent recovery =  $\text{min rec} + \text{max rec} / [1 + \exp((V - V_{1/2})/k)]$ , where min rec and max rec represent the minimum and maximum recovery values,  $V_{1/2}$  represents the voltage corresponding to half-maximal recovery, and  $k$  is a slope factor. Parameters were generated from mean values by curve-fitting algorithms of SigmaPlot, which also provided the asymptotic standard error of each estimate. ND = not determined.

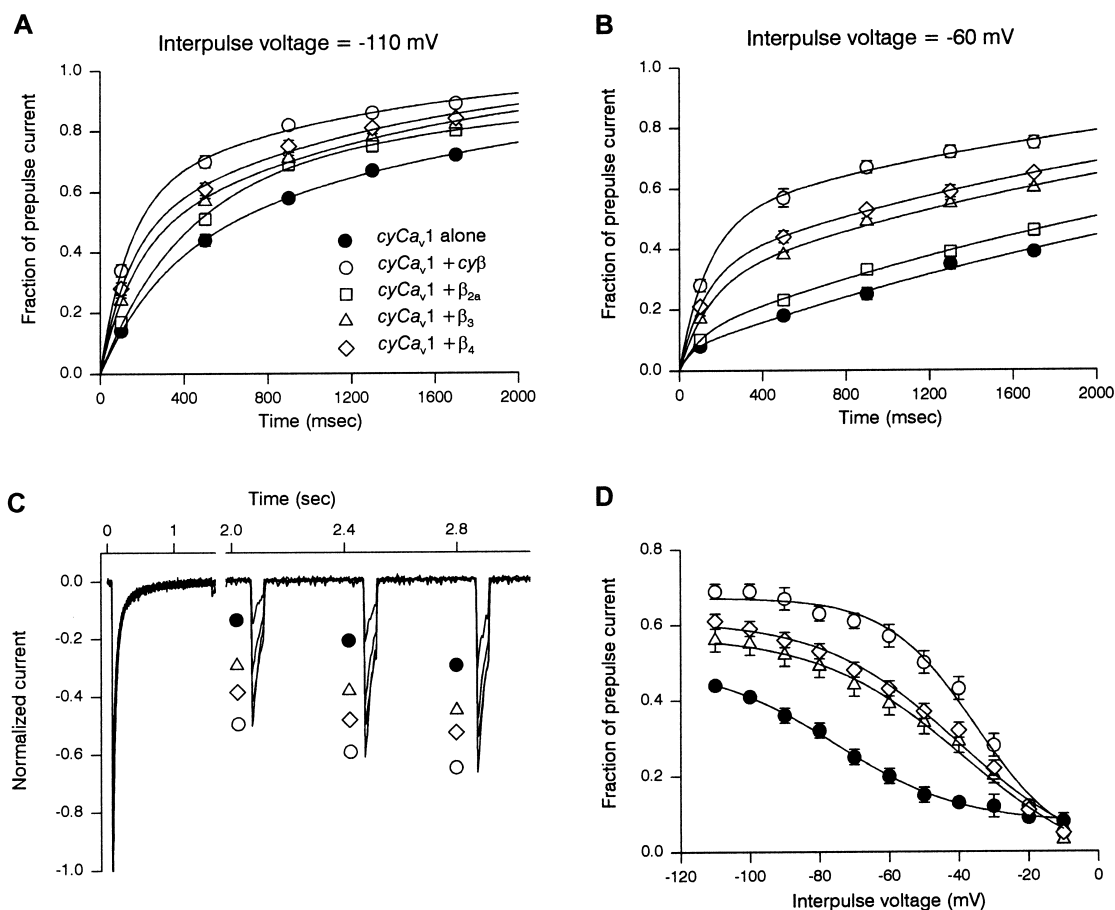


Fig. 2. Recovery of the  $cyCa_v1$  subunit. A: Recovery of  $cyCa_v1$  expressed alone or coexpressed with the  $cy\beta$ ,  $\beta_{2a}$ ,  $\beta_3$ , or  $\beta_4$  subunits. The peak current elicited by the test pulse ( $+10$  mV for 50 ms) after a step of variable duration to  $-110$  mV is shown as the fraction of the peak current elicited by the prepulse ( $+10$  mV for 1500 ms). B: Results of the protocol described in (A) when the interpulse voltage was  $-60$  mV. C: Examples of the recovery of  $cyCa_v1$  expressed alone (closed circles) or in combination with  $cy\beta$  (open circles),  $\beta_3$  (open triangles), or  $\beta_4$  (open diamonds). Oocytes were stepped from a holding voltage of  $-110$  mV to  $+10$  mV for 1500 ms, then hyperpolarized to  $-60$  mV for a variable length of time before a 50 ms test pulse to  $+10$  mV. For each subunit combination, the currents produced by test pulses after interpulse intervals of 500, 900, and 1300 ms are combined into a single sweep to more clearly illustrate the pattern of recovery. Note the difference in time scale between the two halves of the figure. The currents are normalized with respect to the peak current generated by the prepulse. D: Voltage dependence of recovery from inactivation. Following a 1500 ms prepulse to  $+10$  mV, the voltage was stepped to varying voltages for 500 ms before the 50 ms test pulse to  $+10$  mV. Responses are expressed as the fraction of the peak current during the prepulse that was elicited by the test pulse. Symbols are as described in (A).  $n=7-10$  cells for all figures.

$\beta_{2a}$  subunit, which had the weakest effect of the  $\beta$  subunits tested.

Because the interpulse voltage used in this experiment was strongly hyperpolarizing ( $-110$  mV), we examined the possibility that  $\beta$  subunits may not significantly alter the rate of channel recovery when the interpulse voltage is closer to physiological potentials. At an interpulse voltage of  $-60$  mV, the effects of  $\beta$  subunits on recovery were more marked, however, and differences among the various  $\beta$  subunits were more pronounced (Fig. 2B). Examples of recovery of  $cyCa_v1$  after an interpulse potential of  $-60$  mV are shown in Fig. 2C. Recovery of  $cyCa_v1$  was slower after repolarization to  $-60$  mV; although the fast time constant was shorter than that at  $-110$  mV, its contribution to recovery was much smaller (Table 1). The  $cyCa_v1$  subunit expressed alone reached approximately 40% of its peak current after 1600 ms of repolarization, a delay modified only slightly by the  $\beta_{2a}$  subunit, but comparable recovery was seen in the presence of  $\beta_3$  or  $\beta_4$  after 500 ms, and in the presence of  $cy\beta$  after only 200 ms. The

effect of the  $cy\beta$ ,  $\beta_3$ , and  $\beta_4$  subunits was manifested primarily as a greater proportion of recovery accounted for by the fast component.

The difference between the experiments at the two interpulse voltages demonstrated that the effects of  $\beta$  subunits upon recovery from inactivation are voltage-dependent. We investigated the voltage dependence further by measuring recovery after an interpulse of constant length (500 ms) and varying voltage. The results (Fig. 2D) indicate that the effects of  $\beta$  subunits upon recovery of the  $cyCa_v1$  subunit from inactivation are most pronounced at voltages between  $-40$  and  $-80$  mV. The  $cy\beta$ ,  $\beta_3$ , and  $\beta_4$  subunits each shifted the midpoint of the voltage relationship by 25–30 mV as well as raising the maximal degree of recovery (Table 1).

To determine whether the recovery of mammalian  $\alpha_1$  subunits can be similarly modulated, we examined the effects of  $\beta$  subunit coexpression on the human  $Ca_v2.3$  subunit.  $hCa_v2.3$  also exhibits a biexponential pattern of recovery, but the fraction accounted for by the fast component was greater at in-

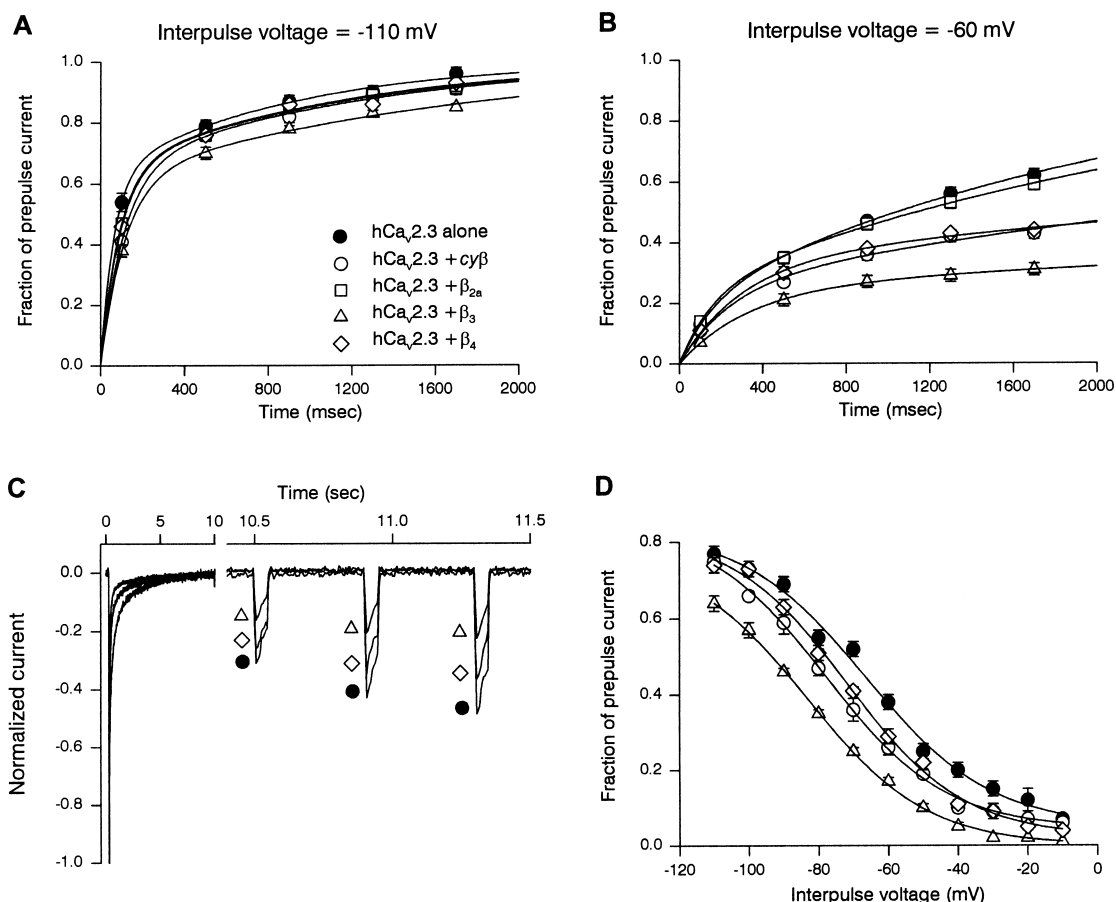


Fig. 3. Recovery of currents carried by the human  $\text{Ca}_v2.3$  subunit. Protocols were as described in Fig. 2, with the exception that a 9.5 s prepulse was used to inactivate the current (16.2 s for the  $\text{Ca}_v2.3+\beta_{2a}$  combination). A: Recovery of  $\text{Ca}_v2.3$  expressed alone or coexpressed with the  $\text{cy}\beta$ ,  $\beta_{2a}$ ,  $\beta_3$ , or  $\beta_4$  subunits after an interpulse of  $-110$  mV. B: Recovery of the subunit combinations shown in (A) after an interpulse of  $-60$  mV. C: Examples of recovery of the  $\text{hCa}_v2.3$  subunit expressed alone (closed circles) or coexpressed with  $\beta_3$  (open triangles) or  $\beta_4$  (open diamonds). The currents shown were elicited by test pulses after a 9.5 s prepulse to  $+10$  mV followed by a 500, 900, or 1300 ms interpulse step to  $-60$  mV. Note the difference in time scale between the two halves of the figure. D: Voltage dependence of recovery. Symbols are as described in (A); the  $\text{hCa}_v2.3+\beta_{2a}$  combination was not tested in this experiment.  $n=4-10$  cells.

terpulse voltages of either  $-110$  or  $-60$  mV. In contrast to  $\text{cyCa}_v1$ , the recovery of  $\text{hCa}_v2.3$  was slowed by coexpression of any  $\beta$  subunit. The effects of the  $\beta$  subunits were minimal at an interpulse voltage of  $-110$  mV (Fig. 3A), but quite evident at  $-60$  mV (Fig. 3B,C), at which the difference among the treatments became more marked after repolarizations of longer duration. At  $-60$  mV,  $\beta_3$  was most effective at slowing recovery, followed by  $\beta_4$  and  $\beta_{2a}$ . The  $\text{cy}\beta$  subunit also slowed recovery in a manner similar to that of  $\beta_4$ . The effects of the  $\beta$  subunits were manifested as an increase in the time constants for each component, although the proportion of recovery accounted for by the fast component was somewhat greater in the presence of a  $\beta$  subunit. The  $\beta$  subunit modulation of recovery was voltage-dependent (Fig. 3D), although to a smaller degree than that seen for  $\text{cyCa}_v1$ , and was reflected as a shift in the midpoint of the recovery curve.

#### 4. Discussion

Previous studies have established several modulatory actions of calcium channel  $\beta$  subunits upon  $\alpha_1$  subunits (for a review see [3]). In addition to its augmentation of  $\alpha_1$  subunit expression in the plasma membrane [17–19] and effects upon

regulation by G proteins or phosphorylation [20], the  $\beta$  subunit shifts the current–voltage relationship and steady-state inactivation of the  $\alpha_1$  subunit, alters the rates of channel activation and inactivation, and affects prepulse facilitation and closed-state inactivation [1,2,21–23]. Here we demonstrate that not only can  $\beta$  subunits also modulate the recovery of the  $\alpha_1$  subunit from inactivation, but that the direction and degree of modulation depend upon the subtypes of both the  $\alpha_1$  and  $\beta$  subunit. Other actions of  $\beta$  subunits vary according to which  $\beta$  subtype is associated with the  $\alpha_1$  subunit. The  $\beta_{1b}$ ,  $\beta_3$ , and  $\beta_4$  subunits accelerate the rate of inactivation of  $\text{hCa}_v2.3$  and shift steady-state inactivation to more hyperpolarized potentials, for example, while the  $\beta_{2a}$  subunit exerts the opposite effects [4,6,22]. The  $\beta_{2a}$  subunit is also unique among mammalian  $\beta$  subtypes in its inability to enhance prepulse facilitation of  $\text{Ca}_v1.2$  [24] or preferential closed-state inactivation of  $\text{Ca}_v2.1$ ,  $\text{Ca}_v2.2$ , and  $\text{Ca}_v2.3$  [23], and in our experiments had the weakest effect upon the recovery of either  $\alpha_1$  subunit from inactivation. Differential modulation by  $\beta$  isoforms is significant in light of the findings that native N-type ( $\text{Ca}_v2.2$ ; [8]), P/Q type ( $\text{Ca}_v2.1$ ; [7]), and neuronal L-type channels ( $\text{Ca}_v1.2$ ,  $\text{Ca}_v1.3$ ; [9]) each contain a clearly identified  $\alpha_1$  subtype, but may include any of three or four of the  $\beta$

isoforms. The association of different  $\beta$  isoforms with a given  $\alpha_1$  subunit does not appear to be random, but varies according to tissue distribution [9] or developmental stage [25].

A surprising finding of these studies was that the direction of modulation differs between the two  $\alpha_1$  subunits. Coexpression of  $\beta$  subunits accelerated recovery of the *cy*Ca<sub>v</sub>1 subunit, but slowed recovery of the hCa<sub>v</sub>2.3 isoform. *cy*Ca<sub>v</sub>1, a homologue of mammalian L-type  $\alpha_1$  subunits, exhibits significant variation in the cytoplasmic loop between domains I and II that contains the primary site for  $\beta$  subunit binding, but is clearly modulated by all three mammalian  $\beta$  subunits studied. Thus, the recovery of mammalian L-type  $\alpha_1$  subunits may be accelerated by certain  $\beta$  subunit isoforms in a similar manner. The degree of modulation exerted by each  $\beta$  subtype also differed between the two  $\alpha_1$  subunits. *cy*Ca<sub>v</sub>1 recovered most quickly in the presence of the *cy* $\beta$  subunit, followed by  $\beta_3$  and  $\beta_4$ , which produced comparable enhancement, and the effect of  $\beta_{2a}$  was seen only at strongly polarized interpulse potentials. In contrast, the  $\beta_3$  subtype had a more marked effect upon the hCa<sub>v</sub>2.3 subunit than  $\beta_4$ , which was similar to *cy* $\beta$ , and  $\beta_{2a}$  had essentially no effect on recovery. The order of potency of the three mammalian  $\beta$  isoforms on the recovery of hCa<sub>v</sub>2.3 is similar to that exerted on preferential closed-state inactivation of the Ca<sub>v</sub>2.2 subunit [23]. Because closed-state inactivation reflects the ease of transition from an intermediate closed state to an inactivated state, whereas recovery from inactivation represents the transition from an inactivated state to a closed state from which the channel can again be activated,  $\beta$  subunits may affect the modulation of the two responses via a similar mechanism.

The interaction between  $\alpha_1$  and  $\beta$  subunits is governed primarily by highly conserved domains in each subunit [26,27], but the present results suggest that modulation of recovery by the  $\beta$  subunit is mediated by a separate interaction site. The three mammalian  $\beta$  subunits studied are nearly identical in peptide sequence within the primary interaction domain, yet their effects upon recovery of the channel vary. The differential effects of  $\beta$  subunits upon inactivation have been linked to two distinct and variable regions external to the primary  $\beta$  interaction domain [4,6], and subtype-specific interaction sites have been found for certain  $\beta$  subunits [28].

Since our experiments were designed to separate recovery from inactivation from other phenomena, such as closed-state inactivation or prepulse facilitation, that can affect the measurement of recovery, we employed extended depolarizing and repolarizing pulses that may not mimic physiological conditions. Nevertheless, the effects of  $\beta$  subunits were evident after interpulses of moderate duration and potential, and are likely to be physiologically relevant. Patil et al. [23], in their description of preferential closed-state inactivation of neuronal calcium channels, argue that calcium channel inactivation may contribute to the synaptic depression seen during a series of action potentials. Differential rates of channel recovery would also affect the availability of channels, leading to altered entry of calcium and effects upon calcium-dependent processes such as docking of synaptic vesicles. The functional importance of recovery from inactivation has been demonstrated by mutations in the human Ca<sub>v</sub>2.1 subunit that are associated with familial hemiplegic migraine. Each of four identified mutations has its most pronounced effects upon the recovery of the channel [15,29]. Alternatively spliced forms of the Ca<sub>v</sub>1.2 subunit also differ in their rate of recovery [30] and

in their sensitivity to the effects of isradipine upon recovery [31]. In addition, the calcium channel  $\gamma$  subunit has recently been shown to slow recovery of the Ca<sub>v</sub>1.2 subunit [32]. Our findings establish that recovery of mammalian calcium channels can also be modulated by  $\beta$  subunits. The differential effects exerted by  $\beta$  subunit isoforms may reflect an additional mechanism by which calcium current heterogeneity is generated in vivo.

*Acknowledgements:* We thank Dr. Edward Perez-Reyes for contributing mammalian Ca<sub>v</sub>2.3,  $\beta_{2a}$ ,  $\beta_3$ , and  $\beta_4$  cDNA clones. This work was supported by NSF Grant IBN-98-08386.

## References

- [1] Lacerda, A.E., Kim, H.S., Ruth, P., Perez-Reyes, E., Flockerzi, V., Hofmann, F., Birnbaumer, L. and Brown, A.M. (1991) *Nature* 352, 527–530.
- [2] Varadi, G., Lory, P., Schultz, D., Varadi, M. and Schwartz, A. (1991) *Nature* 352, 159–162.
- [3] Walker, D. and De Waard, M. (1998) *Trends Neurosci.* 21, 148–154.
- [4] Olcese, R., Qin, N., Schneider, T., Neely, A., Wei, X., Stefani, E. and Birnbaumer, L. (1994) *Neuron* 13, 1433–1438.
- [5] Stea, A., Tomlinson, W.J., Soong, T.W., Bourinet, E., Dubel, S.J., Vincent, S.R. and Snutch, T.P. (1994) *Proc. Natl. Acad. Sci. USA* 91, 10576–10580.
- [6] Qin, N., Olcese, R., Zhou, J., Cabello, O.A., Birnbaumer, L. and Stefani, E. (1996) *Am. J. Physiol.* 271, c1539–c1545.
- [7] Liu, H., De Waard, M., Scott, V.E.S., Gurnett, C.A., Lennon, V.A. and Campbell, K.P. (1996) *J. Biol. Chem.* 271, 13804–13810.
- [8] Scott, V.E.S., De Waard, M., Liu, H., Gurnett, C.A., Venzke, D.P., Lennon, V.A. and Campbell, K.P. (1996) *J. Biol. Chem.* 271, 3207–3212.
- [9] Pichler, M., Cassidy, T.N., Reimer, D., Haase, H., Kraus, R., Ostler, D. and Striessnig, J. (1997) *J. Biol. Chem.* 272, 13877–13882.
- [10] Jeziorski, M.C., Greenberg, R.M. and Anderson, P.A.V. (1999) *Recept. Channels* 6, 375–386.
- [11] Jeziorski, M.C., Greenberg, R.M. and Clark, K.S. (1998) *J. Biol. Chem.* 273, 22792–22799.
- [12] Grabner, M., Bachmann, A., Rosenthal, F., Striessnig, J., Schultz, C., Tautz, D. and Glossmann, H. (1994) *FEBS Lett.* 339, 189–194.
- [13] Neely, A., Olcese, R., Wei, X., Birnbaumer, L. and Stefani, E. (1994) *Biophys. J.* 66, 1895–1903.
- [14] Schneider, T., Wei, X., Olcese, R., Costantin, J.L., Neely, A., Palade, P., Perez-Reyes, E., Qin, N., Zhou, J., Crawford, G.D., Smith, R.G., Appel, S.H., Stefani, E. and Birnbaumer, L. (1994) *Recept. Channels* 2, 255–270.
- [15] Kraus, R.L., Sinnegger, M.J., Glossmann, H., Hering, S. and Striessnig, J. (1998) *J. Biol. Chem.* 273, 5586–5590.
- [16] Zühlke, R.D. and Reuter, H. (1998) *Proc. Natl. Acad. Sci. USA* 95, 3287–3294.
- [17] Chien, A.J., Zhao, X., Shirokov, R.E., Puri, T.S., Chang, C.F., Sun, D., Rios, E. and Hosey, M.M. (1995) *J. Biol. Chem.* 270, 30036–30044.
- [18] Brice, N.L., Berrow, N.S., Campbell, V., Page, K.M., Brickley, K., Tedder, I. and Dolphin, A.C. (1997) *Eur. J. Neurosci.* 9, 749–759.
- [19] Tareilus, E., Roux, M., Qin, N., Olcese, R., Zhou, J., Stefani, E. and Birnbaumer, L. (1997) *Proc. Natl. Acad. Sci. USA* 94, 1703–1708.
- [20] Dolphin, A.C. (1996) *Trends Neurosci.* 19, 35–43.
- [21] Bourinet, E., Charnet, P., Tomlinson, W.J., Stea, A., Snutch, T.P. and Nargeot, J. (1994) *EMBO J.* 13, 5032–5039.
- [22] Jones, L.P., Wei, S.-K. and Yue, D.T. (1998) *J. Gen. Physiol.* 112, 125–143.
- [23] Patil, P.G., Brody, D.L. and Yue, D.T. (1998) *Neuron* 20, 1027–1038.
- [24] Cens, T., Mangoni, M.E., Richard, S., Nargeot, J. and Charnet, P. (1996) *Pflüg. Arch. – Eur. J. Physiol.* 431, 771–774.

- [25] Vance, C.L., Begg, C.M., Lee, W.-L., Haase, H., Copeland, T.D. and McEneaney, M.W. (1998) *J. Biol. Chem.* 273, 14495–14502.
- [26] De Waard, M., Pragnell, M. and Campbell, K.P. (1994) *Neuron* 13, 495–503.
- [27] Pragnell, M., De Waard, M., Mori, Y., Tanabe, T., Snutch, T.P. and Campbell, K.P. (1994) *Nature* 368, 67–70.
- [28] Walker, D., Bichet, D., Geib, S., Mori, E., Cornet, V., Snutch, T.P., Mori, Y. and De Waard, M. (1999) *J. Biol. Chem.* 274, 12383–12390.
- [29] Hans, M., Luvisetto, S., Williams, M.E., Spagnolo, M., Urrutia, A., Tottene, A., Brust, P.F., Johnson, E.C., Harpold, M.M., Stauderman, K.A. and Pietrobon, D. (1999) *J. Neurosci.* 19, 1610–1619.
- [30] Soldatov, N.M., Zühlke, R.D., Bouron, A. and Reuter, H. (1997) *J. Biol. Chem.* 272, 3560–3566.
- [31] Lacinová, L., Klugbauer, N. and Hofmann, F. (2000) *Pflüg. Arch. – Eur. J. Physiol.* 440, 50–60.
- [32] Sipos, I., Pika-Hartlaub, U., Hofmann, F., Flucher, B.F. and Melzer, W. (2000) *Pflüg. Arch. – Eur. J. Physiol.* 439, 691–699.